High-resolution study of the ^{116}Sn(p,t) reaction and shell model structure of ^{114}Sn

P. Guazzoni and L. Zetta
Dipartimento di Fisica dell'Università, and Istituto Nazionale di Fisica Nucleare, Via Celoria 16, I-20133 Milano, Italy

A. Covello and A. Gargano
Dipartimento di Scienze Fisiche, Università di Napoli Federico II, and Istituto Nazionale di Fisica Nucleare, Complesso Universitario di Monte S. Angelo, Via Cintia, I-80126 Napoli, Italy

G. Graw, R. Hertenberger, and H.-F. Wirth
Sektion Physik der Universität München, D-85748 Garching, Germany

M. Jaskola
Soltan Institute for Nuclear Studies, Warsaw, Poland
(Received 6 May 2003; published 27 February 2004)

The ^{116}Sn$(p,t)^{114}$Sn reaction has been studied in a high-resolution experiment at an incident proton energy of 26 MeV. Angular distributions for 61 transitions to levels of ^{114}Sn up to an excitation energy of ~4.1 MeV have been measured. A distorted-wave Born approximation analysis of experimental angular distributions using conventional Woods-Saxon potentials has been done, allowing either the confirmation of previous spin and parity values or the assignment of new spin and parity to a large number of ^{114}Sn states. A shell-model study of ^{114}Sn has been performed using a realistic effective interaction derived from the CD–Bonn nucleon-nucleon potential. The model space has been truncated to states with seniority up to 4. Comparison between the experimental and calculated energy spectra for both positive- and negative-parity states shows a quite satisfactory agreement.

DOI: 10.1103/PhysRevC.69.024619 PACS number(s): 25.40.Hs, 21.10.Hw, 21.60.Cs, 27.60.+j

I. INTRODUCTION

The tin isotopes have long been the subject of both experimental and theoretical studies. In particular, one- and two-neutron transfer reactions have in the past been profitably used to obtain detailed information on the shell-model structure of these nuclei. Because of the major proton shell closure at $Z=50$, it is reasonable to assume that the low-lying states of the tin isotopes can be understood in terms of only $N-50$ neutrons moving in the $1g_{7/2}, 2d_{5/2}, 2d_{3/2}, 3s_{1/2}$, and $1h_{11/2}$ shell-model orbitals. The possibility of understanding nuclear states in terms of neutron degrees of freedom alone has made the tin isotopes a valuable testing ground for shell-model calculations, and for theories that attempt to explain collective phenomena, such as pairing, in terms of shell-model basis states. It is therefore important for our understanding of these basic aspects of nuclear structure that energies, angular momenta, and parities of all low-lying tin states be well determined.

In the past, one- and two-neutron transfer reactions have been profitably used to determine detailed spectroscopic information about these nuclei. The two-neutron transfer reactions (p,t) and (t,p) are particularly valuable in this respect, since these reactions are very sensitive to pairing correlations in the overlap between initial and final states. In recent years, we have undertaken a systematic study of tin isotopes using the (p,t) reaction in high-resolution experiments at the Munich HVEC MP Tandem. We reported the results of this kind of study for ^{120}Sn in a previous paper [1], where they were also compared with the predictions of a realistic shell-model calculation.

In this paper, we have extended our study to the nucleus ^{114}Sn. This nucleus is of special interest since a weak shell closure corresponding to the filling of the lowest single-particle levels $1d_{5/2}$ and $0g_{7/2}$ seems to exist.

The level structure of ^{114}Sn has been evidenced by different sorts of experimental measurements: radioactivity studies from ^{114}In via β^- decay [2] and from ^{114}Sb via β^+ decay [3], inelastic scattering of protons [4], deuterons [5], α particles [6], Coulomb excitation [7,8], in beam γ-ray spectroscopy, with both nonselective and selective reactions, such as $(n,n'\gamma)$ [9], and ^{100}Mo$(^{18}$O$,4n\gamma)$ [10–12], ^{112}Cd$(\alpha,2n\gamma)$ [11,13–16], respectively. Levels in ^{114}Sn have also been studied using one- and two-nucleon transfer reactions ^{115}Sn(d,t) [17], ^{112}Cd$(^3$He$,n)$ [18], ^{112}Sn(t,p) [19], ^{116}Sn(p,t) [20–22], and ^{116}Sn$(\alpha,^6$He$)$ [23]. The results obtained in these works are summarized in the NDS compilation [24], where a more complete list of references can be found.

The $(\mathrm{HI},xn\gamma)$ reactions [10–12] can be classified as high-spin experiments: in fact, the fusion-evaporation reaction mechanism preferably populates states with high alignment and is very selective in high-spin states. On the contrary, two-nucleon transfer reactions at low-excitation energy evidence the correlations arising from the pairing interaction and are complementary to the $(\mathrm{HI},xn\gamma)$, not only in their capability of selecting particular states but also in their spin and parity ranges.

The nucleus ^{114}Sn was measured by means of the two-nucleon transfer reaction ^{116}Sn$(p,t)^{114}$Sn first by Fleming *et al.* [20] at an incident energy of 20 MeV and by Blankert

[21] at 27.5 MeV, with an energy resolution of 25 keV and 14–16 keV, respectively. In the Fleming experiment involving several even Sn isotopes only the most intense transitions were measured, while only partial results of the Blankert experiment were published.

For these reasons we have performed a new investigation of the ^{116}Sn$(p,t)^{114}$Sn reaction by means of a high-resolution experiment to characterize the low-spin states of ^{114}Sn. Differential cross sections of 61 transitions to ^{114}Sn up to an excitation energy of 4136 keV were accurately measured. The angular momentum transfers were determined, and spin and parity assigned to 61 levels.

In connection with the experimental work, we have performed a shell-model study of ^{114}Sn, in which we assume that ^{100}Sn is a closed core and let the valence neutrons occupy the five single-particle levels within the 50–82 shell. To reduce the numerical work required by a complete-basis diagonalization we have resorted to a seniority truncation including states with seniority up to 4. As a two-body interaction between the valence neutrons we have employed a realistic effective interaction derived from the CD-Bonn free nucleon-nucleon (*NN*) potential [25].

The outline of the paper is as follows. In Sec. II we first describe the experimental procedure and then present the results obtained. Section III contains a brief description of our shell-model calculations and the comparison between the calculated and experimental spectra. Section IV presents some concluding remarks.

II. EXPERIMENTAL PROCEDURE AND RESULTS

A. The experiment

The experiment was performed with the 26 MeV proton beam from the Munich HVEC MP Tandem accelerator with a current intensity ranging from 200 up to 300 nA to avoid target heating. The ^{116}Sn isotopic enriched target (^{112}Sn 0.01%, ^{114}Sn 0.01%, ^{115}Sn 0.03%, ^{116}Sn 96.8%, ^{117}Sn 1.5%, ^{118}Sn 0.8%, ^{119}Sn 0.2%, ^{120}Sn 0.5%, ^{122}Sn 0.1%, ^{124}Sn 0.05%) had a thickness of 100 μg/cm^2 on a carbon backing of 5.6 μg/cm^2.

The reaction products were momentum separated by the Q3D magnetic spectrograph, at 11 angles between 6° and 65°: the setting of the spectrograph entrance slits provided for $\theta=5°$ a solid angle of 2.98 msr and for $\theta \geqslant 10°$ a solid angle of 11.04 msr.

The analyzed particles were detected in the 1.8 m long focal plane detector [26], which is a combination of position sensitive proportional wire energy loss detector with additional cathode read out and a rest energy scintillation detector. This device provides focal plane reconstruction and ΔE-E particle identification. The good energetic characteristics of the accelerator, the spectrograph, and the detector allowed for the measurement of high-resolution energy spectra with an energy resolution of about 8 keV full width at half maximum in the detection of the outgoing particles.

The cross section angular distributions were measured in two different magnetic field settings of the spectrograph, in order to reach an excitation energy of the ^{114}Sn residual nucleus of 4136 keV.

The errors in the absolute cross sections are mostly determined by the uncertainties regarding the target thickness, solid angle, and collected charge, giving a systematic error of ~15%, while the dead time was completely negligible.

By means of the computer code AUTOFIT [27] areas and centroids of the triton peaks were determined, using as reference the shape of the peak at 2943 keV.

The very small background, the high resolving power of the magnetic spectrograph, the large solid angle, the favorable peak to background ratio, and the spectrum energy resolution allowed for the observation of rather weakly populated levels; the weakest of them have a cross section of ~1 μb/sr at the maximum in the angular distribution. The energy calibration of the spectra was carried out by using the excitation energy of 13 levels determined in γ-decay experiments [24] and identified also in our triton spectra. The correlation between the measured channels and the excitation energies was performed for the whole range from 0 up to 4136 keV with a polynomial of rank 4. The uncertainty on our quoted energies is estimated at 3 keV.

In Fig. 1 the measured triton spectrum at $\theta=10°$ is shown and the excitation energies for the most excited levels are reported. We have measured 61(p,t) transitions to the final states of ^{114}Sn up to $E_{ex}=4136$ keV, out of which 15 have been observed for the first time.

In Table I all information about previous experiments available in the literature [24] and the results of present transfer reaction experiment are summarized.

B. Experimental results

Starting from a 0^+ initial state and assuming that the neutrons are transferred in a relative $L=0$ state with total spin $S=0$, only natural parity states in the final nucleus will be populated in a one-step transfer process, with a unique L transfer. In this case the determination of the L-transfer directly gives both spin and parity of the observed level.

For the transitions populating the ^{114}Sn states a distorted-wave Born approximation (DWBA) analysis has been carried out, assuming a semimicroscopic dineutron cluster pickup mechanism. The basic assumption is that the relative motion of the transferred spin-singlet neutron pair has zero orbital angular momentum and no radial nodes. The center-of-mass wave function of the transferred neutron pair is then described by a single-particle wave function whose angular momentum equals the total angular momentum L of the transferred pair. The radial dependence of the center-of-mass wave function is obtained by solving the radial Schrödinger equation for the dineutron, requiring that the number of radial nodes, N, is given by the conservation law for three-dimensional harmonic oscillator quanta:

$$Q = 2N + L = \sum_{i=1}^{2} (2n_i + \ell_i),$$

where n_i and ℓ_i are the quantum numbers of the individual nucleon states that form the transferred pair. There is an ambiguity in this prescription when the dineutron pair is composed of shell-model orbitals from different major oscil-

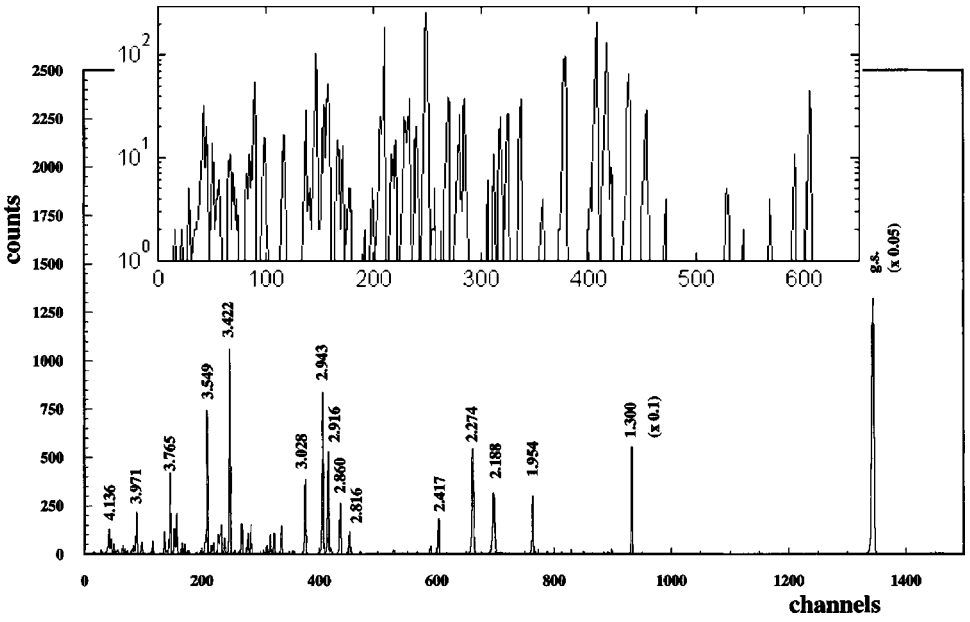

FIG. 1. Position spectrum of tritons measured at $\theta=10°$. The excitation energies of the most prominent peaks are indicated. The inset presents in logarithmic scale the portion of the spectrum between channels 0 and 600 to assess the good quality of the collected data for weakly excited levels.

lator shells, as can happen due to the single-neutron spin-orbit potential. However, the calculated angular distributions are determined mainly by L, and are affected only slightly if N changes by one, and thus this possible ambiguity in N has little effect on our conclusions. In addition to their dependence on L, the shapes of the DWBA angular distributions are dependent on the optical model wells used to determine the proton and triton continuum wave functions, and the kinematics of the entrance and exit channels. These angular distribution shapes depend very little on the detailed microscopic shell-model components of the transferred dineutron cluster. Therefore the DWBA calculations are a valuable guide in the use of the shape of the observed angular distribution to determine the transferred angular momentum L. However, the detailed shell-model structure of the cluster is of great importance in determining the *magnitude* of the transfer cross section. The n_i, ℓ_i values of the components of the cluster are important, as are the relative phases with which these components appear in the cluster. In this paper we use the shell model only to calculate the spectrum of the ^{114}Sn states. The calculation of the shell-model spectroscopic amplitudes and their use together with DWBA transfer amplitudes to determine absolute cross sections [28] for (p,t) reactions on different tin isotopes will be presented in a future publication.

The DWBA calculations have been done in finite-range approximation, using the computer code TWOFNR [29] and a proton-dineutron interaction potential of Gaussian form $V(r_{p2n})=V_0 \exp[-(r_{p2n}/\xi)^2]$ with $\xi=2$ fm. The optical parameters for the proton entrance channel, deduced from a systematic survey of elastic scattering by Perey [30], and for the triton exit channel by Fleming *et al.* [20] have been slightly adjusted for an optimized agreement with the experimental angular distributions.

Table II reports the optical model parameters for the proton and triton continuum wave functions and the geometric parameters used for evaluating the bound-state wave function of the transferred dineutron cluster. The same set of optical model parameters was also used to analyze the angular distributions of the ^{122}Sn$(p,t)^{120}$Sn reaction measured at 20 MeV [20], 26 MeV [1,31], and ^{123}Sb$(p,t)^{121}$Sb reaction measured at 26 MeV [32]. Because of the good agreement achieved between experimental results and DWBA calculations, we assume that two-step processes, which are not taken into account in the present DWBA analysis, are small in this mass region.

Transferred L values have been assigned by comparing the shapes of the experimental angular distributions with the calculated ones. Examples of typical analyses for different L transfers are reported in Figs. 2–7. The clear structure of the angular distributions, allowing for an easy discrimination among different L transfers, is well described by the DWBA calculations. In Fig. 8 the angular distributions of the unresolved levels at 3242, 3515, and 3561 keV are compared with the theoretical estimates. For all the three doublets the percentages of the two different L contributions have been adjusted to obtain the lowest value of χ^2. In the same figure the angular distributions for the excitation of the 7^- state, experimental and theoretical, are also shown.

As Table I evidences, we have made spin-parity assignments for all the observed levels. In particular 15 levels have been observed for the first time and identified in J^π. With respect to the levels reported in NDS [24], 29 confirmations and 7 new assignments of J^π have been made and 4 ambiguities removed. Three unresolved doublets have been also observed, giving 4 confirmations and 2 new assignments. The proposed assignments for the levels observed in the present experiment, new or corresponding to the reported ones in the adopted level scheme [24] with uncertain J^π or without J^π assignment, are discussed in the following together with the unresolved doublets.

2510 keV level. In the adopted level scheme [24] a level is reported at $E_{ex}=2514.760$ keV with spin and parity attribution 3^+ on the basis of a β^+ decay [3] study, ^{112}Cd$(\alpha,2n\gamma)$ ^{114}Sn [11,13,16] and $(n,n'\gamma)$ [9] reaction studies. Furthermore a level at 2513 keV is reported without spin assign-

TABLE I. Columns 1 and 2 give the adopted energies, spins, and parities [24] of the ^{114}Sn levels: columns 3 and 4 the energies, spins, and parities observed in the present work; column 5 gives the integrated cross sections from 5° to 60°. Our quoted energies are estimated to have an uncertainty of ±3 keV. In column 5 absolute cross sections, estimated with a systematic error of ±15%, are reported together with the statistical errors.

^{114}Sn Level scheme				
Adopted		Present experiment		
E_{exc} (keV)	J^{π}	E_{exc} (MeV)	J^{π}	σ_{int} (μb)
0	0^+	0.0	0^+	2492±32
1299.91	2^+	1.300	2^+	520±10
1953.27	0^+	1.954	0^+	17±1
2156.28	0^+	2.154	0^+	1.7±0.3
2187.60	4^+	2.188	4^+	190±4
2238.95	2^+	2.239	2^+	1.0±0.2
2274.99	3^-	2.274	3^-	137±3
2421.67	0^+	2.417	0^+	8.7±0.8
2454.07	2^+	2.451	2^+	6.8±0.7
		2.510	3^-	2.3±0.4
2514.76	3^+			
2576?	2^+	2.576	2^+	1.2±0.2
2614.46	4^+	2.613	4^+	4.9±0.5
2738.4				
2759.7				
2765.36	4^+	2.765	4^+	3.3±0.5
2815.15	5^-	2.816	5^-	22±1
2859.81	4^+	2.860	4^+	51±2
2905.12	4^+			
		2.906	3^-	5.7±0.5
2915.73	2^+	2.916	2^+	85±3
2943.43	2^+	2.943	2^+	125±3
3025	$2,3^+$			
3025.29	0^+	3.028	0^+	24±2
3028.09	$2, 3^+$			
3071.4				
3087.37	7^-	3.088	7^-	10.2±0.7
3100.1				
3107.1				
3149.79	6^+	3.149	6^+	48±2
3186.13	2^+	3.186	2^+	19±1
3188.92	6^+	3.190	6^+	2.0±0.3
3190.39	8^-			
3204	0^+			
3207.61	(2^+)	3.206	4^+	14±1
3211.76	(1,2)			
3226.00	$2^+,3^+$			
		3.225	3^-	4.7±0.6
3242.05	5^-			
		3.242	5^-+6^+	4.6±0.6
3244.39	6^-			
3308.4	0^+	3.309	0^+	8.7±0.9

TABLE I. (*Continued.*)

^{114}Sn Level scheme				
Adopted		Present experiment		
E_{exc} (keV)	J^{π}	E_{exc} (MeV)	J^{π}	σ_{int} (μb)
3326.50	2^+	3.325	2^+	17±1
3357.42	4^+	3.358	4^+	114±3
3363.00	4^-,5^-,6^-	3.363	5^-	1.4±0.2
3364.8				
3380.1				
3392.1				
3393.0				
3396.1				
3396.9	(4^-)	3.397	6^+	4.4±0.3
3422.7	0^+	3.422	0^+	51±2
3448.37		3.448	4^+	9.6±0.9
3451.8		3.452	0^+	1.4±0.2
3471.4	6^+	3.473	6^+	52±2
3478.85	(2^+)	3.477	2^+	10.2±0.3
		3.486	5^-	17±1
3510.70	9^-			
		3.515	3^-+9^-	20±2
3514.19	2^+,3^+			
3525.36	3^-	3.526	3^-	7.6±0.8
3548	0^+	3.549	0^+	40±2
3561.1	2^+			
		3.561	2^++7^-	32±2
3566.47	7^-			
		3.587	4^+	4.3±0.7
3610.71	$5(^-)$			
3658.7		3.654	4^+	3.5±0.6
		3.680	4^+	3.2±0.6
3685.15	6^-			
3690		3.696	2^+	8.9±0.8
3717.83	7^-			
3720.4				
3722	2^+	3.727	2^+	33±2
3740.03		3.740	0^+	14±1
3759	0^+	3.765	0^+	23±1
3781.98	2^+			
		3.786	4^+	8.0±0.8
		3.800	2^+	15±1
3854.3				
3855.6				
		3.871	5^-	5.9±0.6
3871.28	8^+			
3871.3	2^+	3.876	2^+	1.6±0.2
3889.3				
3928				
		3.939	3^-	9.7±0.9

TABLE I. (*Continued.*)

^{114}Sn Level scheme				
Adopted		Present experiment		
E_{exc} (keV)	J^{π}	E_{exc} (MeV)	J^{π}	σ_{int} (μb)
3956	2^+			
		3.971	2^+	34±2
3971.21	8^-			
3976				
3987.6		3.988	3^-	7.3±0.8
3991.39	$2^+,3^+,4^+$			
		4.000	4^+	77±0.8
4029.83	$2^+,3^+,4^+$			
4043.15	5^-			
		4.044	5^-	5.4±0.6
4046.82	5^-			
		4.057	6^+	11±1
4088.74	8^+			
		4.095	2^+	4.5±0.5
4119	4^+	4.118	4^+	9.3±0.9
4136		4.136	4^+	38±2

ment from the ^{116}Sn$(p,t)^{114}$Sn reaction measurement [21]. In our experiment the level at 2510 keV is quite weakly populated and the angular distribution is compatible with an $L=3$ transfer and a $J^{\pi}=3^-$ attribution. This level most probably cannot coincide with the level reported in NDS [21] at $E_{ex}=2514.760$ keV.

2906 keV level. In the adopted level scheme [24] a level is reported at $E_{ex}=2905.12$ keV with spin and parity attribution 4^+ on the basis of a β^+ decay [3], (t,p) [19] and $(n,n'\gamma)$ [9] studies. In the present experiment the 2906 keV level is not so strongly populated and the angular distribution is reasonably well reproduced by $L=3$ transfer. The present assignment is $J^{\pi}=3^-$. This level might not correspond to the state reported in NDS at $E_{ex}=2905.12$ keV [24].

3225 keV level. In NDS compilation [24] a level is given at an energy of 3226.00 keV with spin and parity assignment of 2^+ and 3^+ deduced from β^+ decay [3] and $(n,n'\gamma)$ [9] measurement. In our study the level at 3225 keV is quite well reproduced by $L=3$ transfer and the present assignment is $J^{\pi}=3^-$. Presumably this level does not coincide with the level at 3226.00 keV.

3242 keV level. On NDS [24] there are two levels with energies 3242.05 keV and 3244.39 keV and with $J^{\pi}=5^-$ and $J^{\pi}=6^-$, respectively, from ^{112}Cd$(\alpha,2n\gamma)^{114}$Sn and $(n,n'\gamma)$ reactions. Our measured angular distribution is well reproduced by assuming that this transition corresponds to an unresolved doublet of one level with $J^{\pi}=5^-$ ($L=5$ transfer 5%) and another level with $J^{\pi}=6^+$ ($L=6$ transfer 95%).

3397 keV level. The adopted level scheme [24] reports four levels at $E_{ex}=3392.1$, 3393.0, 3396.1 keV without spin and parity assignment, and 3396.9 keV identified in the ^{112}Cd$(\alpha,2n\gamma)^{114}$Sn reaction [11,13,16] with (4^-) assignment. In our study the angular distribution is consistent with $L=6$ transfer and the present assignment is $J^{\pi}=6^+$.

3448 keV level. In Ref. [24] a level is listed at an energy of 3448.37 keV on the basis of an $(n,n'\gamma)$ [9] study without spin and parity assignment. In our experiment the level at 3448 keV is quite reasonably populated and we reproduce quite well the measured angular distribution with $L=4$ transfer. The present assignment is $J^{\pi}=4^+$.

3452 keV *level*. The NDS [24] report a level at an energy of 3451.8 keV observed in an $(n,n'\gamma)$ [9] study without spin

TABLE II. The Woods-Saxon optical model parameters for the incident proton, the outgoing triton, and the geometrical parameters for the bound state (BS) of the transferred dineutron cluster.

	V_r (MeV)	r_r (fm)	a_r (fm)	W_v (MeV)	r_v (fm)	a_v (fm)	W_d (MeV)	r_d (fm)	a_d (fm)	V_{so} (MeV)	r_{so} (fm)	a_{so} (fm)	r_c (fm)
p	50.0	1.25	0.65				10.0	1.30	0.60	3.00	1.25	0.70	1.25
t	176.0	1.14	0.72	18.0	1.61	0.82				8.00	1.10	0.80	1.30
BS		1.30	0.50										

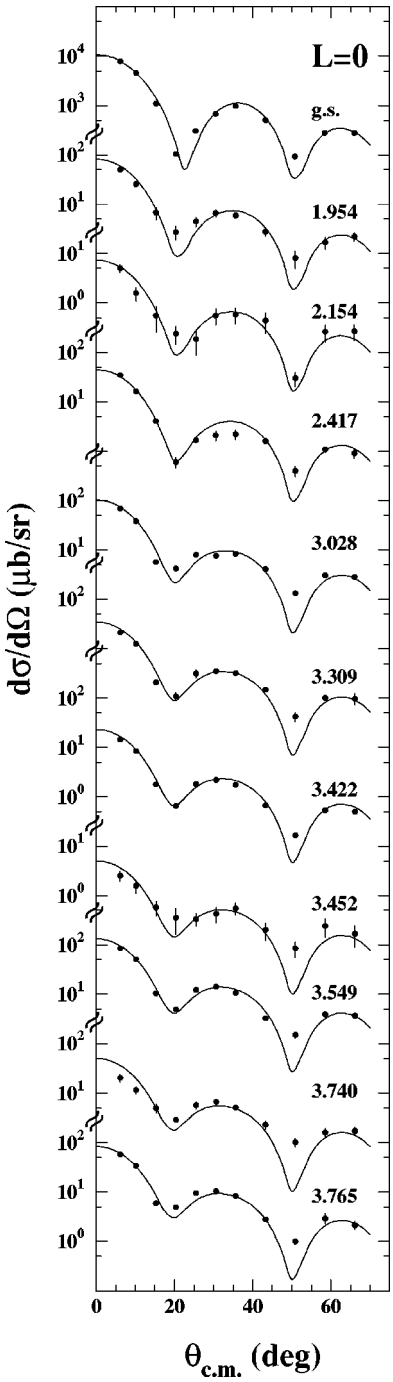

FIG. 2. Differential cross sections for the excitation of 0^+ states by the ^{116}Sn$(p,t)^{114}$Sn reaction. The full curves are from DWBA calculations. The energies attributed to the observed levels are those given in the present work.

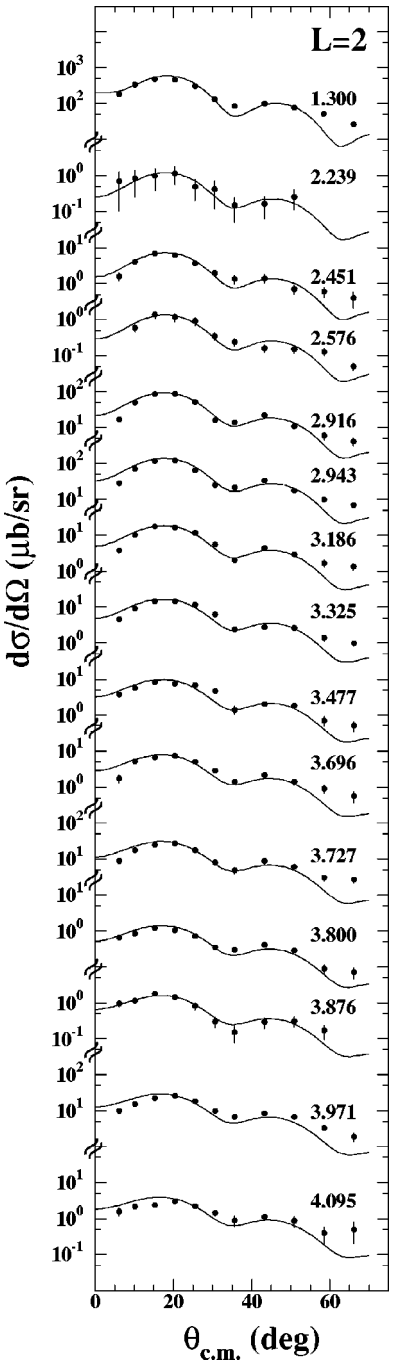

FIG. 3. Differential cross sections for the excitation of 2^+ states by the ^{116}Sn$(p,t)^{114}$Sn reaction. The full curves are from DWBA calculations. The energies attributed to the observed levels are those given in the present work.

and parity assignment. In our case the level, quite weakly populated, is well reproduced by $L=0$ transfer and we assign $J^\pi=0^+$ to this level.

3486 keV level. At this energy no level is given in the adopted level scheme [24]. This level is strongly populated and the angular distribution is reasonably well reproduced by $L=5$ transfer. The present assignment is $J^\pi=5^-$.

3515 keV level. In the adopted level scheme [24] there are two levels, the first at 3510.70 keV with $J^\pi=9^-$ and the second one at 3514.19 keV identified in an $(n,n'\gamma)$ [9] study with $J^\pi=2^+$ and 3^+. We reproduce the angular distribution quite well by considering an unresolved doublet with $J^\pi=3^-(5\%)$ and $J^\pi=9^-(95\%)$.

3561 keV level. In Ref. [24] two levels are reported, one at 3561.1 keV derived from an $(n,n'\gamma)$ [9] study with $J^\pi=2^+$ and another one at 3566.47 keV, $J^\pi=7^-$. We observe a strongly populated transition and reproduce the angular dis-

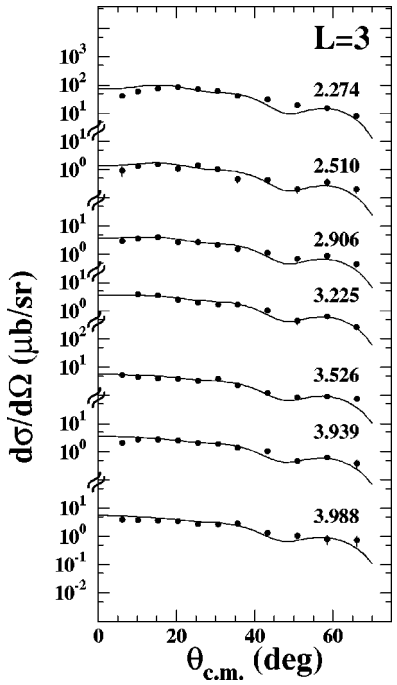

FIG. 4. Differential cross sections for the excitation of 3^- states by the ^{116}Sn$(p,t)^{114}$Sn reaction. The full curves are from DWBA calculations. The energies attributed to the observed levels are those given in the present work.

tribution by considering an unresolved doublet with $J^\pi = 2^+(7\%)$ and $J^\pi = 7^-(93\%)$.

3587 keV level. At this energy no level is given in the adopted level scheme [24]. In our experiment this level is weakly populated. The measured angular distribution is consistent with an attribution of $J^\pi = 4^+$.

3654 keV level. In the adopted level scheme [24] a level is given at 3658.7 keV on the basis of $(\alpha, n\gamma)$ reaction without spin and parity assignment. In our study this level is well reproduced by $L=4$ transfer and we attribute $J^\pi = 4^+$.

3680 keV level. At this energy no level is given in the adopted level scheme [24]. In our measurement this level is quite weakly populated and the angular distribution is compatible with the attribution $J^\pi = 4^+$.

3696 keV level. In the adopted level scheme [24] a level is given at 3690 keV on the basis of (p,t) reaction study [21] without spin and parity assignment. In our case we reproduce the angular distribution quite well by $L=2$ transfer. Therefore, the present assignment is $J^\pi = 2^+$.

3740 keV level. In the adopted level scheme [24] a level is reported at 3740.03 keV derived from an $(n,n'\gamma)$ [9] study, without spin and parity assignment. We reproduce the angular distribution of this strongly populated level by $L=0$ transfer. Present attribution is $J^\pi = 0^+$.

3786 keV and 3800 keV levels. At these energies no levels are given in the adopted level scheme [24]. We reproduce the angular distributions of these levels by considering $L=4$ and 2 transfers, respectively. Present assignments for these levels are $J^\pi = 4^+$ and $J^\pi = 2^+$, respectively.

3871 keV and 3876 keV levels. In the adopted level scheme [24] two levels are reported at 3871.28 keV, $J^\pi = 8^+$, from ^{112}Cd$(\alpha, 2n\gamma)^{114}$Sn, (HI, $xn\gamma$), and ^{100}Mo$(^{18}O, 4n\gamma)$ ^{114}Sn reaction studies and at 3871.3 keV, $J^\pi = 2^+$, from (p,t) reaction. In our experiment the angular distributions are compatible with an $L=5$ and 2 transfers, respectively. On this basis we assign $J^\pi = 5^-$ and $J^\pi = 2^+$, respectively. Presumably while the level at 3871 keV does not correspond to the level quoted at 3871.28 keV, the level at 3876 keV coincides with the level quoted at 3871.3 keV.

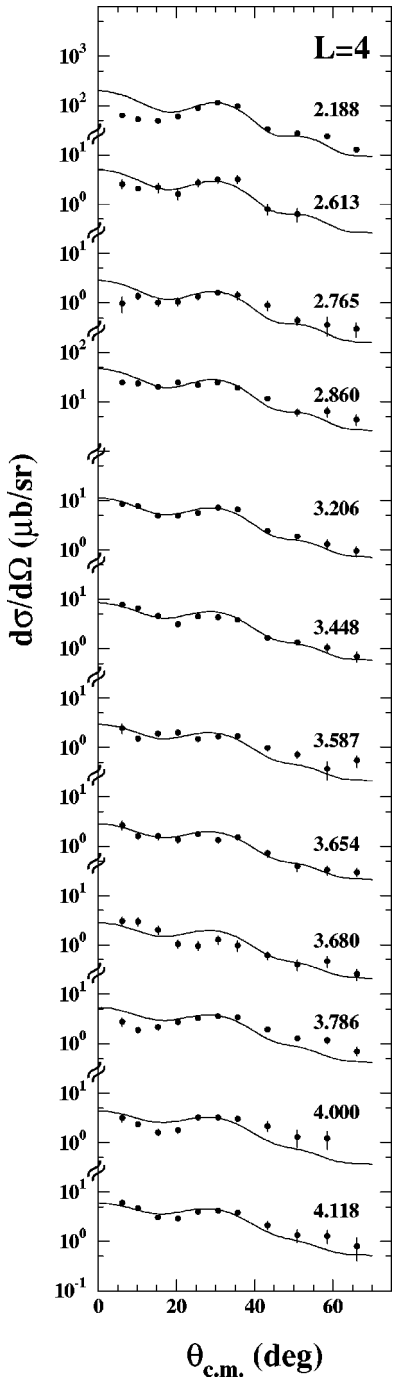

FIG. 5. Differential cross sections for the excitation of 4^+ states by the ^{116}Sn$(p,t)^{114}$Sn reaction. The full curves are from DWBA calculations. The energies attributed to the observed levels are those given in the present work.

3939 keV level. At this energy no level is given in the

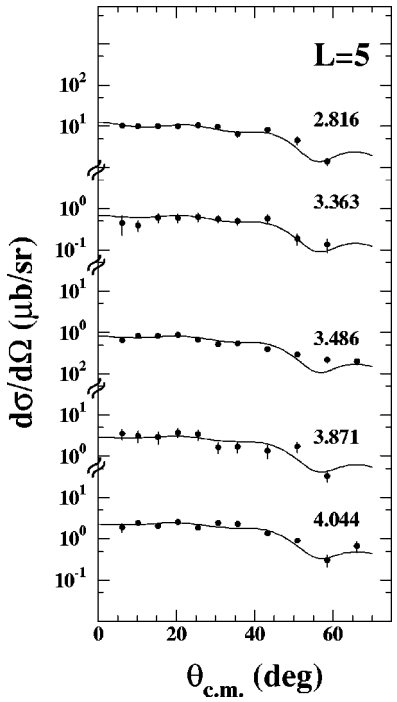

FIG. 6. Differential cross sections for the excitation of 5^- states by the ^{116}Sn$(p,t)^{114}$Sn reaction. The full curves are from DWBA calculations. The energies attributed to the observed levels are those given in the present work.

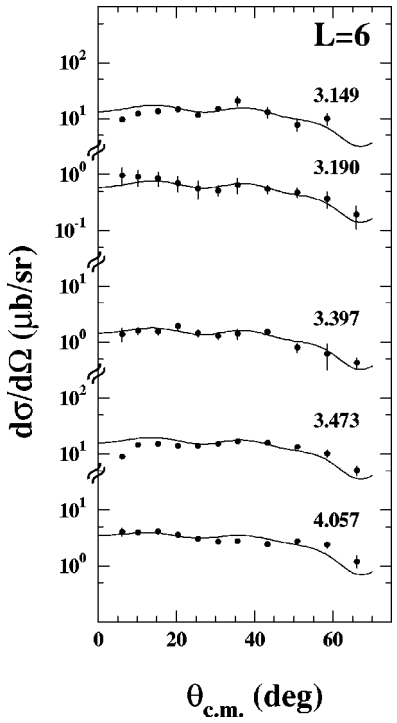

FIG. 7. Differential cross sections for the excitation of 6^+ states by the ^{116}Sn$(p,t)^{114}$Sn reaction. The full curves are from DWBA calculations. The energies attributed to the observed levels are those given in the present work.

adopted level scheme [24]. In our experiment the angular distribution is compatible with an $L=3$ transfer, and on this basis we assign $J^\pi=3^-$.

3971 keV level. In the adopted level scheme [24] two levels are given at 3971.21($J^\pi=8^-$) and 3976 keV, the latter found in (p,t) reaction without spin and parity assignment [21]. In our case this level, corresponding to the adopted 3976 keV level, is quite strongly populated and the angular distribution is reasonably well reproduced by $L=2$ transfer. Present assignment is $J^\pi=2^+$.

3988 keV level. In the adopted level scheme [24] a level is reported at 3987.6 keV without spin and parity assignment. In our measurement the shape of the angular distribution is quite well reproduced by $L=3$ transfer. Present assignment is $J^\pi=3^-$.

4000 keV, 4057 keV, and 4095 keV levels. At these energies no levels are listed in the adopted level scheme [24]. In our case the shape of the angular distributions is quite well reproduced by $L=4$, 6, and 2 transfers, respectively. Present assignments for these levels are $J^\pi=4^+$, $J^\pi=6^+$, and $J^\pi=2^+$, respectively.

4136 keV level. A level at 4136 keV from (p,t) experiment by Blankert *et al.* [21] is reported on the adopted level scheme [24], without spin and parity assignment. In our analysis a reasonable reproduction of the angular distribution is obtained assuming an $L=4$ transfer. Present assignment is $J^\pi=4^+$.

III. SHELL-MODEL CALCULATIONS

Our shell-model study of ^{114}Sn is along the same lines of that performed for ^{120}Sn [1]. We assume that ^{100}Sn is a closed core and let the 14 valence neutrons occupy the single-particle (SP) levels $0g_{7/2}$, $1d_{5/2}$, $1d_{3/2}$, $2s_{1/2}$, and $0h_{11/2}$. To reduce the size of the energy matrices to be set up and diagonalized, we have found it convenient to resort to a seniority truncation. This we have made by means of an approach which is based on a chain calculation across nuclei differing by two in nucleon number. This method, which we call chain-calculation method (CCM), has the advantage to make it possible to further reduce the seniority-truncated

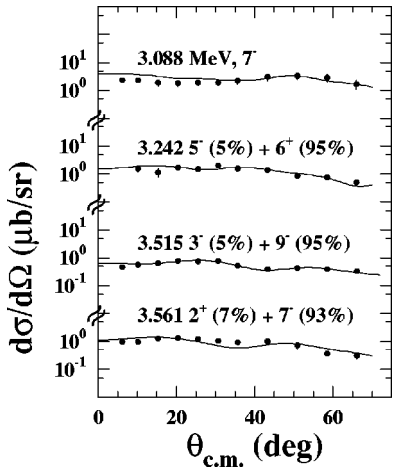

FIG. 8. Differential cross sections for the excitation of the 7^- state and three unresolved doublets by the ^{116}Sn$(p,t)^{114}$Sn reaction. The full curves are from DWBA calculations. The energies attributed to the observed levels are those given in the present work.

shell-model spaces without significant loss in the accuracy of the results. A description of the CCM can be found in Refs. [1,33]. Consistent with our previous study of ^{120}Sn, we have included here states with seniority $v \leqslant 4$.

As two-body interaction between the valence particles, we employ an effective neutron-neutron interaction $V_{\rm eff}$ derived from the CD-Bonn free *NN* potential [25]. The latter fits very accurately the *NN* data below 350 MeV. Our derivation of $V_{\rm eff}$ is based on a *G*-matrix folded diagram method and is described in Ref. [34], which also contains a list of relevant references. Here, $V_{\rm eff}$ represents the interaction between two-valence neutrons outside the doubly closed ^{100}Sn and may not be completely adequate for systems with several valence particles, as is the case of ^{114}Sn. Actually, we have found that the calculated excitation energies go in the right direction when weakening the matrix elements of $V_{\rm eff}$. More precisely, it turns out that the agreement between theory and experiment is substantially improved by reducing the $J^\pi = 0^+$ matrix elements by a factor of 0.9.

Our adopted values for the SP energies are the following (in MeV): $\epsilon_{g_{7/2}} = 0.0$, $\epsilon_{d_{5/2}} = 0.35$, $\epsilon_{s_{1/2}} = 2.1$, $\epsilon_{d_{3/2}} = 2.4$, and $\epsilon_{h_{11/2}} = 3.5$. These have been obtained by taking the average values of the SP energies needed to reproduce the energies of the first four experimental excited states in ^{113}Sn and ^{115}Sn, which are, together with the $1/2^+$ ground state, predominantly of one-particle nature in both nuclei. As compared to the set of SP energies adopted for ^{120}Sn [1], the main differences are the decrease of $\epsilon_{d_{5/2}}$ by about 250 keV and the increase of $\epsilon_{h_{11/2}}$ by about 500 keV. In this context, it is worth noting that from the theoretical study of light tin isotopes, Ref. [34], it is seen that no major changes in the SP energies are needed when approaching doubly magic ^{100}Sn. In fact, the only new feature is the inversion of the $d_{5/2}$ and $g_{7/2}$ levels, which is in agreement with the findings of most shell-model calculations.

To start with, we compare the calculated excitation energies of the yrast states with the experimental ones [24]. In fact, these states are likely to be dominated by configurations with $v \leqslant 4$, and, as a consequence, they allow us to test the two-body matrix elements of $V_{\rm eff}$ as well as the adopted SP energies. This comparison is made in Fig. 9, where we see that the discrepancies go from few keV to about 250 keV, with the exception of the 2^+ and 3^- states. Concerning the former, which we predict to lie at 380 keV above the experimental one, it is worth noting that also for the light Sn isotopes the 2^+ excitation energies are overestimated by our calculations [34]. A higher discrepancy (about 800 keV) occurs for the 3^- state, but this is not surprising since configurations outside the chosen model space are likely to be important in this case. In summary, the agreement between theory and experiment may be considered quite satisfactory. In this connection, it may be mentioned that the quality of our results is comparable to that obtained in the work of Ref. [35], where a similar calculation was performed with a surface δ interaction.

We now compare the excitation energies measured in the present experiment with the calculated values. This comparison is made in Figs. 10 and 11 for positive- and negative-parity states, respectively. In these figures we do not report the 0^+ and 3^- states, since any attempt to establish a correspondence between calculated and experimental levels may be misleading.

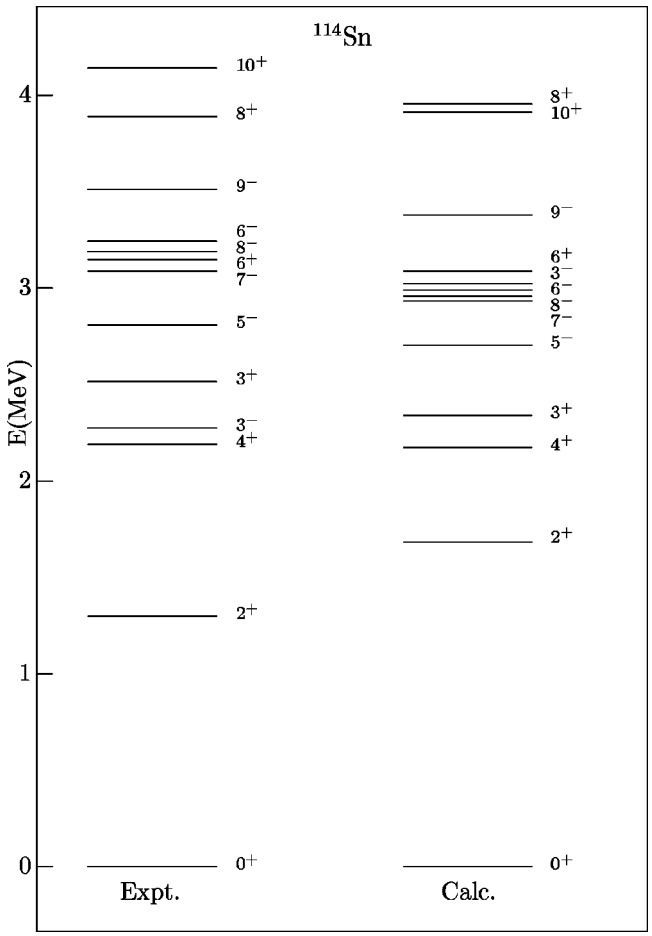

FIG. 9. Experimental and calculated yrast states in ^{114}Sn.

We first discuss the results presented in Fig. 10. In the present experiment 16 2^+ levels have been populated up to 4.095 MeV. These can be associated with the 16 lowest calculated 2^+ states, the differences between the theoretical and experimental excitation energies ranging from a few to about 300 keV, the only exception being the yrast state which, as discussed above, is overestimated by 380 keV. As for the 4^+ states, our calculations reproduce the observed level density (14 levels in the energy interval 2.2–4.2 MeV). We may also attempt an identification of the experimental levels with the theoretical ones, but above 3.5 MeV the discrepancies reach 500 keV for some states. Finally, the first two observed 6^+ states are very well reproduced by our calculations, while the discrepancies for the energies of the other four 6^+ states go from 500 to 600 keV.

Let us now come to Fig. 11. As already pointed out, a good agreement between theory and experiment is found for the energies of the yrast levels. The observed energies of the three 5^- states above the yrast one are also well reproduced by our calculations, the discrepancy being less than 200 keV. For the second excited 7^- state and the two highest-lying 5^-

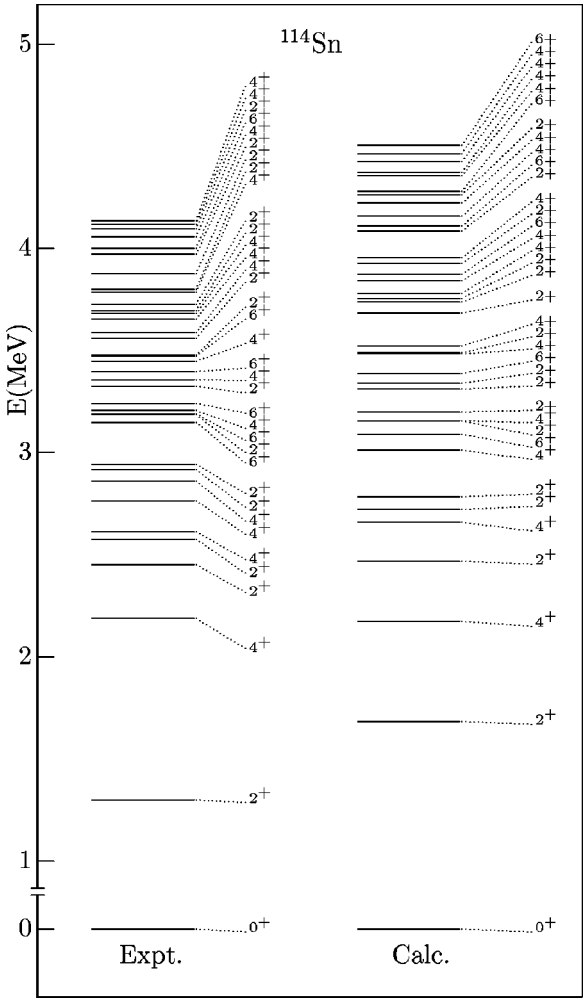

FIG. 10. Experimental and calculated positive-parity states in ^{114}Sn.

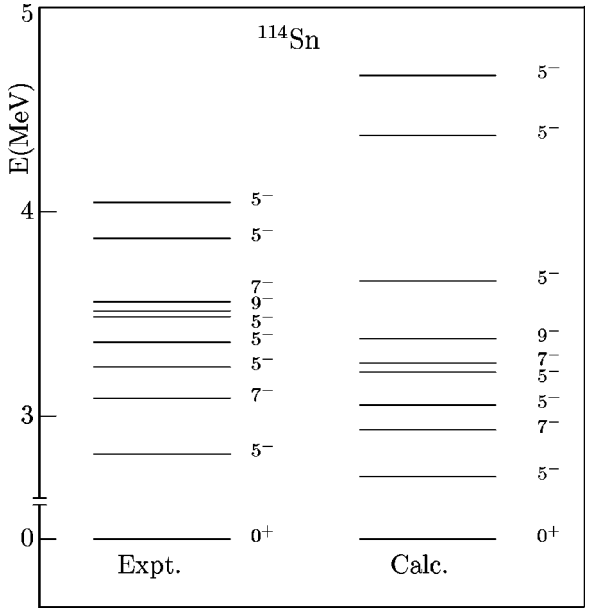

FIG. 11. Experimental and calculated negative-parity states in ^{114}Sn.

states a larger discrepancy is found, which ranges from 300 to 600 keV.

As a general remark regarding both positive- and negative-parity spectra, we point out that the discrepancies between theory and experiment may be partially attributed to the lack of configurations with $v>4$, which are likely to produce a down-shift of most of the high-lying levels.

IV. SUMMARY

In a high-resolution experiment we measured 61 transitions to levels of ^{114}Sn up to an excitation energy of 4.136 MeV via the (p,t) reaction induced by 26 MeV incident proton energy on ^{116}Sn.

A DWBA analysis of the experimental angular distributions has been carried out assuming a semimicroscopic dineutron cluster pickup mechanism. The calculations have been performed in finite range approximation.

The clear structure of the angular distributions allowed for the discrimination among different L transfers and, consequently, for an improvement of the knowledge of the ^{114}Sn level scheme. In fact, we have assigned spin and parity to 15 new levels, and removed the uncertainty in spin-parity assignments to four states.

Along with the experimental work, we have performed a shell-model study of ^{114}Sn truncating the model space to states with $v\leqslant 4$. As two-body interaction between the valence neutrons we have used an effective interaction derived from the CD-Bonn nucleon-nucleon potential. While no adjustable parameter appears in the calculation of our two-body matrix elements, we have obtained a significant improvement in the agreement between experiment and theory by slightly reducing (10%) the $J^{\pi}=0^{+}$ matrix elements.

We have made a comparison between the states observed in the present experiment and those predicted by the theory, with the exception of the $J^{\pi}=0^{+}$ and 3^{-} states. The theoretical results lend support to the experimental findings. In particular, the observed level density is reproduced for all the considered values of J^{π}. A one-to-one correspondence between calculated and observed levels has been established, although with discrepancies that reach 600 keV above 3.5 MeV excitation energy.

In conclusion, the results of the present work, together with those of Ref. [1], confirm that the shell model is the main theoretical framework for the description of tin isotopes. A companion study of ^{110}Sn is currently under way.

ACKNOWLEDGMENTS

We wish to thank Professor Ben Bayman for the enlightening suggestions. This work was supported in part by a grant of the Italian CRUI and German DAAD under Programma Vigoni. The work at the University of Naples Federico II was supported in part by the Italian Ministero dell'Istruzione, dell'Università e della Ricerca (MIUR).

[1] P. Guazzoni, M. Jaskóla, L. Zetta, A. Covello, A. Gargano, Y. Eisermann, G. Graw, R. Hertenberger, A. Metz, F. Nuoffer, and G. Staudt, Phys. Rev. C **60**, 054603 (1999).
[2] H. E. Bosch, M. Behar, M. C. Cambiaggio, G. Garcia Bermudez, and L. Szybisz, Can. J. Phys. **51**, 2260 (1973).
[3] M. E. Wigmans, R. J. Heynis, P. M. A. van der Kam, and H. Verheul, Phys. Rev. C **14**, 229 (1976).
[4] A. Backlin, W. Dietrich, R. Julin, J. Kantele, M. Luontama, and L. Westerberg, Phys. Lett. **62B**, 402 (1976).
[5] Y. S. Kim and B. L. Cohen, Phys. Rev. **142**, 788 (1966).
[6] G. Bruge, J. C. Faivre, H. Faraggi, and A. Bussiere, Nucl. Phys. **A146**, 597 (1970).
[7] A. Backlin, N. G. Jonsson, R. Julin, J. Kantele, M. Luontama, A. Passoja, and T. Poikolainen, Nucl. Phys. **A351**, 490 (1981).
[8] N. G. Jonsson, A. Backlin, J. Kantele, R. Julin, M. Luontama, and A. Passoja, Nucl. Phys. **A371**, 333 (1981).
[9] S. Yu. Araddad, A. M. Demidov, M. M. Dyufani, V. A. Kurkin, J. M. Rateb, and S. M. Zlitni, Izv. Akad. Nauk SSSR, Ser. Fiz. **54**, 1824 (1990).
[10] H. Harada, M. Sugawara, M. Kusakari, H. Shinohara, Y. Ono, K. Furuno, T. Hosoda, M. Adachi, S. Matsuki, and N. Kawamura, Phys. Rev. C **39**, 132 (1989).
[11] M. Schimmer, S. Albers, A. Dewald, A. Gelberg, R. Wirowski, and P. von Brentano, Nucl. Phys. **A539**, 527 (1992).
[12] J. Gableske, A. Dewald, H. Tiesler, M. Wilhelm, T. Klemme, O. Vogel, I. Schneider, R. Peusquens, S. Kasemann, K. O. Zell, P. von Brentano, P. Petikov, D. Bazzacco, C. Rossi Alvarez, S. Lunardi, G. de Angelis, M. de Poli, and C. Fahlander, Nucl. Phys. **A691**, 551 (2001).
[13] A. Van Poelgeest, J. Bron, W. H. A. Hesselink, K. Allaart, J. J. A. Zalmstra, M. J. Uitzinger, and H. Verheul, Nucl. Phys. **A346**, 70 (1980).
[14] M. Schimmer, R. Wirowski, S. Albers, G. Bohm, A. Gelberg, and P. von Brentano, Z. Phys. A **338**, 117 (1991).
[15] M. Schimmer, R. Wirowski, and P. von Brentano, Nucl. Phys. **A569**, 458 (1994).
[16] R. Wirowski, M. Schimmer, L. Esser, S. Albers, K. O. Zell, and P. von Brentano, Nucl. Phys. **A586**, 427 (1995).
[17] E. J. Schneid, A. Prakash, and B. L. Cohen, Phys. Rev. **156**, 1316 (1967).
[18] R. E. Anderson, C. D. Zafiratos, D. A. Lind, F. E. Cecil, H. H. Wieman, and W. P. Alford, Nucl. Phys. **A281**, 389 (1977).
[19] H. J. Bjerregaard, O. Hansen, O. Nathan, R. Chapman, and S. Hinds, Nucl. Phys. **A131**, 481 (1969).
[20] D. G. Fleming, M. Blann, H. W. Fulbright, and J. A. Robbins, Nucl. Phys. **A157**, 1 (1970).
[21] P. J. Blankert, Ph.D. thesis, Vrije University of Amsterdam, 1979.
[22] E. Gerlich, J. Guillot, H. Langevin-Joliot, J. Van de Wiele, S. Gales, G. Duhamel, G. Perrin, C. P. Massolo, and M. Sakai, Phys. Rev. C **39**, 2190 (1989).
[23] E. Gerlich, J. Guillot, H. Langevin-Joliot, S. Gales, M. Sakai, J. Van de Wiele, G. Duhamel, and G. Perrin, Phys. Lett. **117B**, 20 (1982).
[24] J. Blachot, Nucl. Data Sheets **97**, 593 (2002).
[25] R. Machleidt, Phys. Rev. C **63**, 024001 (2001).
[26] E. Zanotti, M. Bisenberger, R. Hertenberger, H. Kader, and G. Graw, Nucl. Instrum. Methods Phys. Res. A **310**, 706 (1991).
[27] J. R. Comfort, ANL Physics Division, Informal Report PHYS–1970B, 1970.
[28] B. Bayman (private communication).
[29] M. Igarashi, computer code TWOFNR, 1977.
[30] F. G. Perey, Phys. Rev. **131**, 745 (1963).
[31] G. Cata-Danil, P. Guazzoni, M. Jaskóla, L. Zetta, G. Graw, R. Hertenberger, D. Hofer, P. Schiemenz, B. Valnion, E. Zanotti-Mueller, U. Atzrott, F. Hoyler, F. Nuoffer, and G. Staudt, J. Phys. G **22**, 107 (1996).
[32] P. Guazzoni, M. Jaskóla, V. Yu. Ponomarev, L. Zetta, G. Graw, R. Hertenberger, and G. Staudt, Phys. Rev. C **62**, 054312 (2000).
[33] A. Covello, F. Andreozzi, L. Coraggio, A. Gargano, and A. Porrino, in *Contemporary Nuclear Shell Models*, Lecture Notes in Physics Vol. 482 (Springer-Verlag, Berlin, 1997).
[34] F. Andreozzi, L. Coraggio, A. Covello, A. Gargano, T. T. S. Kuo, Z. B. Li, and A. Porrino, Phys. Rev. C **54**, 1636 (1996).
[35] M. Schimmer, R. Wirowski, and P. von Brentano, Nucl. Phys. **A587**, 465 (1995).